
TOWARD RELIABLE SIGNALS DECODING FOR ELECTROENCEPHALOGRAM: A BENCHMARK STUDY TO EEGNeX

A PREPRINT

Xia Chen ^{* a}

Xiangbin Teng^b

Han Chen^c

Yafeng Pan^c

Philipp Geyer^d

July 26, 2022

ABSTRACT

The development of brain-computer interfaces (BCI) has facilitated our study of mental representations in the brain. Neural networks (NNs) have been widely used in BCI due to their decent pattern learning capabilities; however, to our best knowledge, a comprehensive comparison between various neural network models has not been well addressed, due to the interdisciplinary difficulty and case-based study in the domain. Here, we tested the capabilities of common NN architectures in deciphering mental representations from electroencephalogram (EEG) signals, which were recorded in representative classification tasks. In this study, we: 1. Construct 20 mechanism-wise different, typical NN types and their variants on decoding various EEG datasets to show a comprehensive performance comparison regarding their EEG information representation capability. 2. Lighten an efficient pathway based on the analysis results to gradually develop general improvements and propose a novel NN architecture: EEGNeX. 3. We open-sourced all models in an out-of-the-box status, to serve as the benchmark in the BCI community. The performance benchmark contributes as an essential milestone to filling the gap between domains understanding and support for further interdisciplinary studies like analogy investigations between the brain bioelectric signal generation process and NN architecture. All benchmark models and EEGNeX source code is available at: <https://github.com/chenxiachan/EEGNeX>.

1 Introduction

The Brain-Computer Interface (BCI) study aims to research in communication pathway between machine and brain signals [Wolpaw et al., 2000]. From the perspective of information theory, today's machine learning models, especially Neural Networks [Schmidhuber, 2015], are increasingly similar to the human brain in many tasks [Hasson et al., 2020]: a universal structure to process, store and communicate input/output data that carries information. In this context, recent research has incorporated NNs into the BCI domain for feature extraction. Among all neuroimaging methods, one of the most widely used in BCI is electroencephalography (EEG) [Niedermeyer and da Silva, 2005] because EEG recording is non-invasive and of low risk and low cost. Instead of taking inputs like images, videos, or languages, NNs are also able to accept and process EEG signals without any prior knowledge to aid in understanding the human brain.

With the strength of feature extraction and representation learning ability, accuracy advantages in decoding EEG have been well proved in various NN types of variations. Throughout domain literature reviews, general Recurrent Neural

^aLeibniz University Hannover, Germany <xia.chen@iek.uni-hannover.de>

^bDepartment of Education and Psychology, Freie Universität Berlin, 14195 Berlin, Germany

^cDepartment of Psychology and Behavioral Sciences, Zhejiang University, China

^dLeibniz University Hannover, Germany

Networks (RNNs, primarily referring to Long Short-Term Memory, LSTM [Hochreiter and Schmidhuber, 1997]; and Gated Recurrent Unit, GRU [Chung et al., 2014]) [Ruffini et al., 2016, Craik et al., 2019], Convolutional Neural Networks (Conv. or CNNs) [Alzubaidi et al., 2021, Altaheri et al., 2021], and domain integrated structures like EEGNet [Lawhern et al., 2018], own dominant part of adaptation in the EEG community. In spite of the widespread research, we realize that there is a certain gap that exists in the community: Most studies focus primarily on enhancing classification accuracy on a particular dataset or a type of task by incorporating manual feature extraction via domain knowledge preprocessing [Craik et al., 2019], regularization [Deng et al., 2021], or incorporate data with signal transformation techniques [Huang et al., 2020, Altaheri et al., 2021]. Furthermore, most studies usually claim different NN architectures and data preprocessing procedures with fine hyperparameter tuning models, making understanding the generalization performance of representation learning abilities among different deep learning models difficult. Thus, it remains unclear how those previous approaches perform in the same context and can be used to guide for further improvement. In other words, in this paper, we try to answer the following two questions:

- *How well do different types of neural network models extract features from raw EEG data?*
- *How to design an efficient neural network for representation learning in the BCI domain?*

To address these questions, we make contributions in this paper in a three-fold way:

1. We conducted a large-scale performance benchmark on different deep learning models' accuracies for EEG classification tasks. The comparison results revealed EEG-based information representation capability of different NN types of forms.
2. Based on the benchmark results, we provide a trajectory from an advanced NN architecture, namely, EEGNet, to EEGNeX. The new architecture achieves more accurate classification performance tested in diverse EEG datasets/tasks with benchmark models.
3. We open-source all benchmark models and EEGNeX to bring a testbed for research, and aim to reduce the difficulties of NN implementation in the BCI domain.

The remainder of this paper is organized as follows: Target datasets, different neural networks, and accuracy benchmark results are described, followed by a benchmark analysis (Section 2). Section 3 presents the structural innovation roadmap based on EEGNet and validates the performance novelty of new model: EEGNeX. Section 4&5 discuss the future direction and conclude. Figure 1 illustratively summarizes the objective of this study.

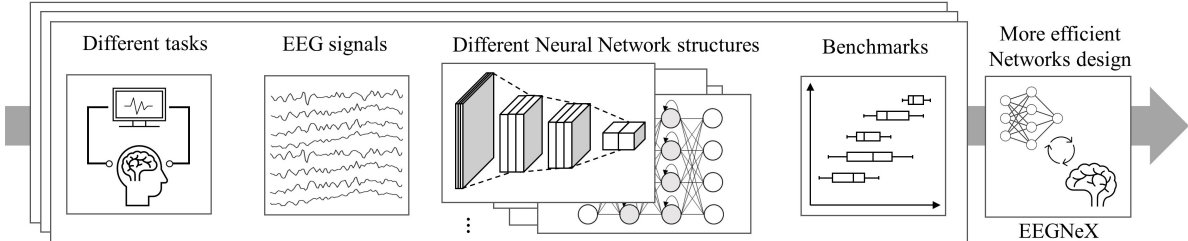


Figure 1: Overall visualization of the research pipeline; We implement different NN architects into variate EEG-based, BCI classification tasks in open-source. Based on the benchmark results, this study aims to alleviate the difficulty of finding the path to adapt NNs efficiently toward higher accuracy in the domain. In the end, a novel NN: EEGNeX structure is proposed with validation.

2 Materials and Methodologies

2.1 Related research

In this subsection, a brief review of the two major NN adaptations and their development into the EEG classification domain is described, followed by a parallel analogy of the NN development in their own original domain.

In tasks of EEG-based classification, the first well-known NN approach was ConvNet which used two convolutional layers for extracting temporal and spatial features with dense layers applied on a P300 task [Cecotti and Graser, 2010]. A similar CNN-based approach with max pooling layers [Schirrmeister et al., 2017] is applied and shows a

performance advantage when compared with a well-known, advanced domain-knowledge-based algorithm - filterbank common spatial patterns (FBCSP) [Chin et al., 2009]. EEGNet is based on the previous methods and further uses a combination of depthwise convolution with separable convolution [Lawhern et al., 2018]. With dropout layer, batch normalization layers, kernel constraint, and max pooling stride, EEGNet claimed to have fewer parameters and more robust cross-sections performance than ShallowConvNet (with two convolution layers) and DeepConvNet (with five convolution layers). Due to the robustness and advanced performance implementation of EEGNet, several extended variations that combine domain knowledge are proposed. For example, Incep-EEGNet [Riyad et al., 2020] extended EEGNet by applying multi-head convolutions as an inception block with different kernel sizes (receptive fields) and pointwise convolution. By applying different narrow filter banks to the original signal with integration, FBCNet presents a hybrid approach with performance improvement on motor imagery (MI) tasks [Mane et al., 2021].

For RNN-based models, less attention has been drawn to the research of EEG-based classification tasks [Craik et al., 2019]. A two-layers LSTM implementation is used for emotion recognition and achieves a performance advantage compared to statistical-based feature selection methods with traditional machine learning classifiers [Alhagry et al., 2017]. Similar LSTM implementations with feature extractors in MI tasks reported better performance than traditional methods and other deep networks, including CNN [Wang et al., 2018]. The other RNN variant, GRU, combined with the attention mechanism [Vaswani et al., 2017] has been applied to the emotion classification task [Chen et al., 2019]. The result shows that the GRU model with attention performs better than CNN and LSTM. Subsequently, a structure that combines CNN and LSTM is proposed for the same task with faster training time, in which CNNs are used to handle the spatial information from the EEG while RNNs extract the temporal information [Wilaiprasitporn et al., 2019].

Originally, CNN and RNN were primarily developed as classical models for tasks such as speech recognition (Natural Language Processing, NLP, temporal) and computer vision (CV, spatial) domain, individually. The first intersection between them appears when the attention-based RNN Transformer, namely, BERT [Devlin et al., 2018] is proposed in language translation and ViT [Dosovitskiy et al., 2020] in image recognition. Although ViT performs better than traditional CNN architectures, e.g., VGGNet [Simonyan and Zisserman, 2014], ResNet [He et al., 2016], EfficientNet [Tan and Le, 2019], the discussion of the advantages of such hybrid NN architectures is still ongoing: ConvNeXt [Liu et al., 2022] fine-adjusted the ResNet architecture to further improve the CNN-based models to reach the level of Transformers in terms of accuracy and scalability while maintaining the simplicity and efficiency of standard convolution networks. In general, those models' performance in a way, represents their information processing levels. For BCI, which aims to interpret implicit information from brain activities, examining and making efforts to investigate different NNs' information representation processes, and learn from their development experiences in the domain are significant.

2.2 Data Description: MNIST of BRAIN DIGITS

To conduct a comprehensive and in-depth investigation of EEG representation learning and feature extraction capabilities on different NNs, we chose a large, complex, and single-subject EEG multiclassification dataset: *MindBigData* [Vivancos]. This open database contains four different devices, 1,207,293 brain signals of 2 seconds long each. The signal records the imagine of presented digit images after exposing a subject to the visual stimulus of the MNIST dataset (from 0 to 9, -1 represents noise), resulting in similar phase synchrony among multiple channels for all classes. As the sign-to-noise ratio of EEG signals is relatively low, NNs must avoid memorizing the noise components from EEG signals to end up overfitting the dataset.

In this paper, Emotive EPOC devices data with 14 channels of EEG signals were selected for benchmarking. The raw EEG signals were recorded at a sample rate of 128 Hz; there are around 6500 trials for each digit image, with each trial containing 256 timesteps for 14 channels. We conducted a simple and common data preprocessing strategy: 1. Noise events removal (-1); 2. A combination of Butterworth lowpass filter (with a cutoff frequency of 63Hz) and a notch filter at 50Hz is applied on all trial; 3. The first 32 timesteps (250ms) for each trial are trimmed to avoid noises caused by sensor power on; 4. Data MinMax scaling (between 0-1) with standardization.

The dataset was grouped according to events (records of all channels for one event), and then were randomly divided into three parts: 80% training set, 10% validation set, and 10% test set.

2.3 Benchmark Methods

We focus on implementing performance benchmarking among different NN structures regarding their architectures and ability of EEG feature extraction. We selected four major layer types and their variations available from TensorFlow [Abadi et al., 2016]: 2D convolution layer, 1D convolution layer, LSTM layer, GRU layer, and a combined implementation - ConvLSTM2D for benchmarking. Following the thorough-out EEG domain reviews [Craik et al., 2019, Hosseini et al., 2020], we also reproduced common architectural and well-proved regulation procedures:

- Using kernel regularizers in RNNs.
- Using a CNN layer and batch normalization [Ioffe and Szegedy, 2015] with exponential linear unit (ELU) activation function [Shah et al., 2016] as a standard CNN component.
- Adding average/max pooling layers at the final layer of CNN to account for local translation invariance.

Furthermore, we also selected several trending variants of CNNs whose mechanisms might affect the representation learning ability of NNs, including:

- Depthwise separable convolutions [Chollet, 2017], which consist of first performing a depthwise spatial convolution (which acts on each input channel separately) followed by a pointwise convolution that mixes the resulting output channels.
- Causal padding, originally designed in WaveNet [Oord et al., 2016] for sequential sound generation, as an implementation option in the 1D convolution layer. It pads the layer's input with zeros in the front so that we can also predict the values of early time steps.
- Dilation, convolution with a wider kernel created by regularly inserting spaces between the kernel elements to gain more global features.

A reproduction of EEGNet is integrated into the benchmark. In this study, we chose EEGNet-8,2, because its performance is better than EEGNet-4,2 (8 and 4 stand for different filter numbers of the first convolution layer in EEGNet), based on results from the original paper [Lawhern et al., 2018]. The detailed architecture of all benchmark NNs is available in Appendix.

To ensure that different modeling structures present their own best performance, all benchmark methods were run under the same two-stage scheme: 1. With the training set under the batch size of 128 for each epoch with default learning rate (0.01), the trained model accuracy is monitored on the validation set. The learning rate is reduced by half when accuracy stops improving for five epochs. The training process stops when there is no improvement for 20 epochs in the validation set to prevent overfitting; 2. Evaluate model performance by running on the test set. This two-stage strategy is designed to avoid data leakage and represent the performance of all benchmark models in the real-world production environment.

An open-source code in Keras is provided for easy, out-of-box reproduction to use in different research sources (<https://github.com/chenxiachan/EEGNeX>). All models are coded in the same implementation format with input in the shape of (*trials* * *channels* * *timesteps*), and one-hot-encoded output. We designed an experiment to run all models on the dataset for ten rounds with random seeds to record their accuracy performances for statistic tests.

2.4 Benchmark Results

Figure 2 presents the performance result across all the models. Table 1 supplements their key feature information. Based on the interpretation of benchmark results, we extracted some valuable pieces of information:

- EEGNet presents the best performance among all benchmark models.
- In RNN-based models, GRU performs better than LSTM with fewer parameters required.
- NN architectures designed to process sequences are not ideal for EEG feature extraction and representation (RNNs and CNN with causal structure). Compared with RNNs, CNN structure shows higher overall accuracy.
- In the basic structure of CNNs, separable 2D convolution architecture owns the best EEG feature extraction and representation ability. The accuracy stability is enhanced with the combination of depthwise-separable 2D convolution.

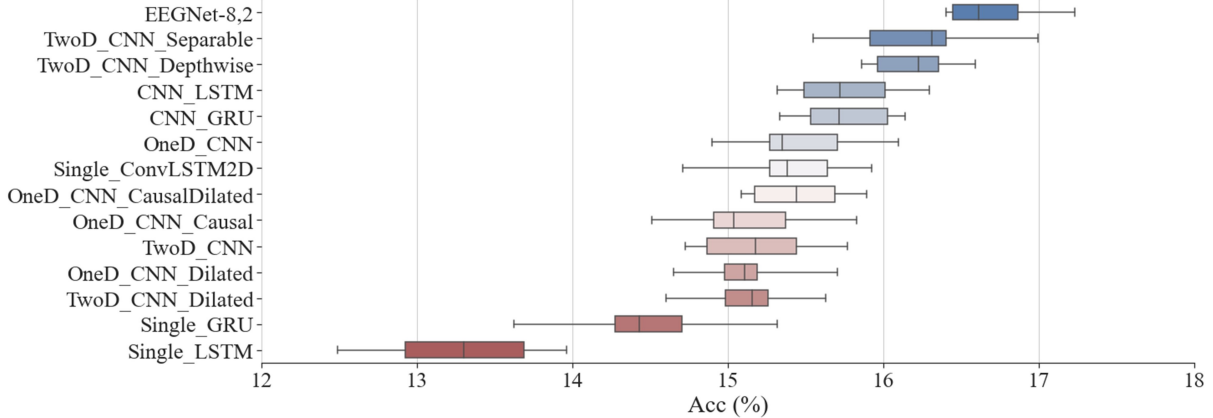


Figure 2: Results of 10-round model classification performance benchmark for the MindBigData dataset sampled all folds and all subjects. Each boxplot bar illustrates the median with an interquartile range (25th and 75th percentiles) and two standard errors of the mean in each error bar. In general, CNN-based structures outperform RNN-based models in accuracy.

Model Name	Accuracy	Deviation	Trainable Para.	non-trainable Para.
Single_LSTM	13.129	0.432	301,910	0
Single_GRU	14.733	0.349	230,110	0
OneD_CNN	15.355	0.212	94,870	384
OneD_CNN_Dilated	15.147	0.427	88,470	384
OneD_CNN_Causal	15.725	0.409	114,070	384
OneD_CNN_CausalDilated	15.738	0.273	114,070	384
TwoD_CNN	16.010	0.439	120,342	256
TwoD_CNN_Dilated	15.027	0.326	107,542	256
TwoD_CNN_Separable	16.445	0.298	76,470	384
TwoD_CNN_Depthwise	17.046	0.337	73,334	704
CNN_LSTM	16.200	0.293	1,532,310	384
CNN_GRU	16.615	0.299	1,179,990	384
Single_ConvLSTM2D	16.386	0.382	299,478	128
EEGNet-8,2	17.493	0.293	3,386	1,008
EEGNet*	17.527	0.313		

Table 1: The key features of benchmark models. The average accuracy and deviation are calculated based on 10 rounds of the train-validation process with random seeds in the data split. In addition, model parameter sizes are presented along to represent the network complexity and search space size. An open-source version (<https://github.com/vlawhern/arl-eegmodels>) of EEGNet (with mark *) is included in the benchmark.

- Performance of hybrid model structures (CNN-LSTM, CNN-GRU) owns a considerable accuracy improvement over any single model.

To conclude this section, we found that it is less effective to design a network fit for temporal feature extraction instead of spatial in the multiclassification task of EEG signal decoding. Due to the built-in inductive biases of CNN-based structures, they own more flexibility toward implicit information translation equivariance. Furthermore, the network design involves cross-channel spatial filtering would significantly enhance the performance. All advantageous design components can be found in EEGNet, as: 1. The first part – the 2D convolution layer extracts the spectral representation of EEG input; 2. The second part – the kernel size of depthwise 2D convolution is tailored to the number of channels and directed to perform convolutions across channels. 3. The third part – separable 2D convolution conducted as feature extraction & learning. By revisiting the three parts mentioned above and adapting to modern network component designs, we can modify the EEGNet toward higher general performance.

3 Roadmap: from EEGNet to EEGNeX

In this section, we provide a trajectory going from an EEGNet to an EEGNeX that adopts findings from the last section, as well as some key component implementations of ConvNeXt [Liu et al., 2022]. The roadmap starts from a standard EEGNet with the adjustment of network architecture in different parts. Sequentially, component changes at the micro level are tested in the fixed network structure. We set the EEGNet as the backbone and tracked the successful steps tested on the same dataset with performance improvement on average over five rounds. The summarized roadmap is as followed: 1) Reinforce the spectral representation extraction from EEG input, 2) wider convolutions in the general architecture, 3) Pooling layer removal, 4) Inverse bottleneck structure, and 5) various micro adjustments. The detailed procedure with the results of each step is illustrated in Figure 3.

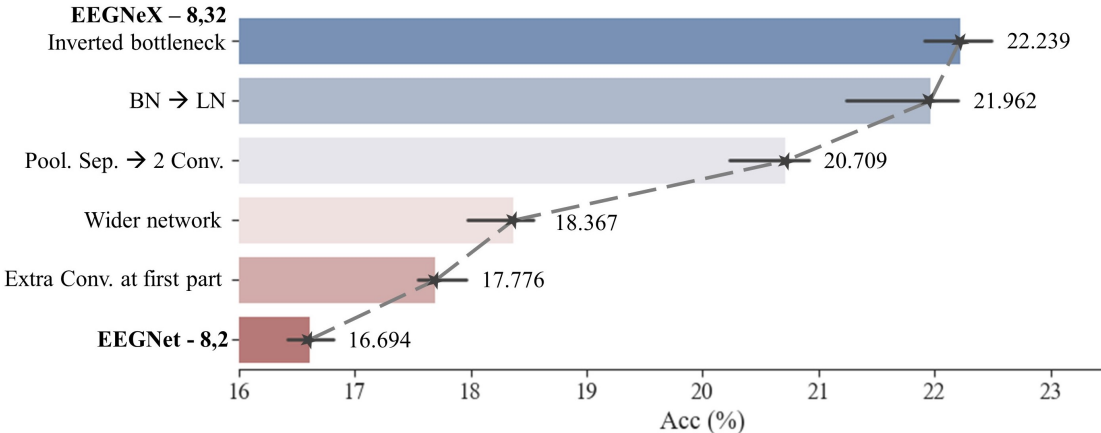


Figure 3: The roadmap of modifying from EEGNet - 8,2 toward EEGNeX - 8,32. The bars record the five times average performance of the model at each step. The black horizontal lines represent the deviation to reflect model performance stability. In the end, our pure convolutions network structure, namely EEGNeX, outperforms the EEGNet - 8,2 by 33% on the MindBigData dataset.

3.1 Thicken the first part of spectral information extraction

Based on the study from Section 2, we noticed that the current structure of EEGNet is designed in three parts with the particular purpose of information processing. The first part that aims to extract spectral information from EEG input is shallow, with only one layer of 2D convolutions. Considering the general network layer depth shouldn't be too deep, we added one more standard CNN block into the first part, consisting of a 2D convolution with same batch normalization layer and an ELU activation layer. This improves the accuracy from 16.7% to 17.8%. It is worth mentioning that the adjustment we offered is the most intuitive solution, and a more optimal design in this part is likely to exist.

3.2 Wider network

Depthwise convolutions are first proposed to use parameters more efficiently in the network that is trained with a large image dataset [Howard et al., 2017]. The advantage is in two-fold: 1. The built-in mechanism acts as a cross-channel, frequency spatial learner (see Figure 4, subfigure c), which improves the global feature extraction abilities, especially adopted in multi-channel EEG. 2. It reduces network parameters and complexity; however, the EEG decoding domain normally deals with a dataset by using a shallower network structure compared to typical CNNs in the CV domain (ResNet, EfficientNet). The reduced parameters would lead to a too small network to properly learn during training. In this study, we expand the width of the network by two to reconcile this issue. The accuracy is improved by this adjustment from 17.8% to 18.4%.

3.3 Replace the separable convolution and pooling layers with two 2D convolutions

In this step, we focus on the third part of EEGNet and arise two design considerations regarding separable convolution and pooling layers:

- Intuitively, separable convolution is a method to factorize a convolution kernel into two smaller kernels [Howard et al., 2017]. It consists of a depthwise convolution (cross channels) and a pointwise convolution (1*1 convolution to combine the outputs of the depthwise convolution). Since the channel dimension is reduced to one from the previous process, separable convolution is redundant.
- Pooling layer is designed initially to: 1) reduce network parameters and calculation difficulty, 2) prevent overfitting, and 3) enhance the invariance of the network [Scherer et al., 2010]. Essentially, it is a feature selection process but contributes less to accuracy improvement. The pooling mechanism filters out partial information as a compromise to less training cost that is considered in the CV domain when dealing with large datasets. As mentioned in the previous step, the worry in our domain is more concerned if there are too less parameters in the network instead of too many.

To adopt both considerations, we referred to step one and replaced the separable convolution in the third part of EEG with two standard CNN blocks. We also removed average pooling layers separable convolutions (1*8). To reproduce pooling sampling process, we added dilatation in both the CNN blocks, 1*2, and 1*4, respectively. This step brings a further gain from 18.4% to 20.7%.

3.4 Replace batch normalization with layer normalization

Followed by the suggestion from ConvNeXt, we substitute all batch normalization layers in the network. This process improves the result slightly by 1.3% to 22.0%.

3.5 Inverted bottleneck

Based on the design of advanced CNN architectures [Sandler et al., 2018, Tan and Le, 2019], we modified the network blocks to the inverted bottleneck structure with an expansion ratio of 4. The final output filters of CNN blocks are 8*32*32*8. At this point, the performance reaches 22.2%. We also noticed that this design contributes to enhancing the model performance stability.

Closing remarks We propose a new architecture of the network design after a few more rounds of micro adjustments. Instead of the successful changes mentioned above, some experiences that failed in improvement are as follows:

1. Deeper networks: By simply stacking more convolution layers usually leads to converging difficulty in the training phase with poor performance. Compared with image data, EEG datasets are smaller size-wise. A deep network would earlier confront the overfitting issue.
2. Fewer normalization and/or activation layers: The modern CNN-based structures in the computer vision domain achieve some improvements by removing some normalization or activation layers. The experience is not applicable in our domain; the reason lies in the shallow network design.
3. Reordering different parts/layers: We also tried various combinations of parts' orders based on the structure of EEGNet. No improvements were found.

Ultimately, we present a pure convolution network – EEGNeX that adapts to modern design experience. The final accuracy on the same dataset with an average accuracy of 22.2%, achieving a significant improvement compared with EEGNet by 33%. The fixed structure of EEGNeX with full parameter description is presented in Figure 4 and Table 2.

3.6 Evaluation Datasets

In this section, we applied EEGNeX and all benchmark models as candidates in a broader data scope to validate the general feature extraction & representation performance. Besides the MindBigData, we tested on three diverse EEG datasets with the consideration of covering different tasks, classes, trial lengths, data sizes, and channels number:

- OpenMBI Data: A 2-class Motor-Imagery (MI) data from Korea University EEG dataset [Lee et al., 2019].
- BCIC-IV-2A Data: A 4-class MI data from BCI Competition IV Dataset 2A [Tangermann et al., 2012].
- Feedback Error-Related Negativity: A 2-class Event-Related Potential (ERP) data from BCI Challenge hosted by Kaggle [Margaux et al., 2012].

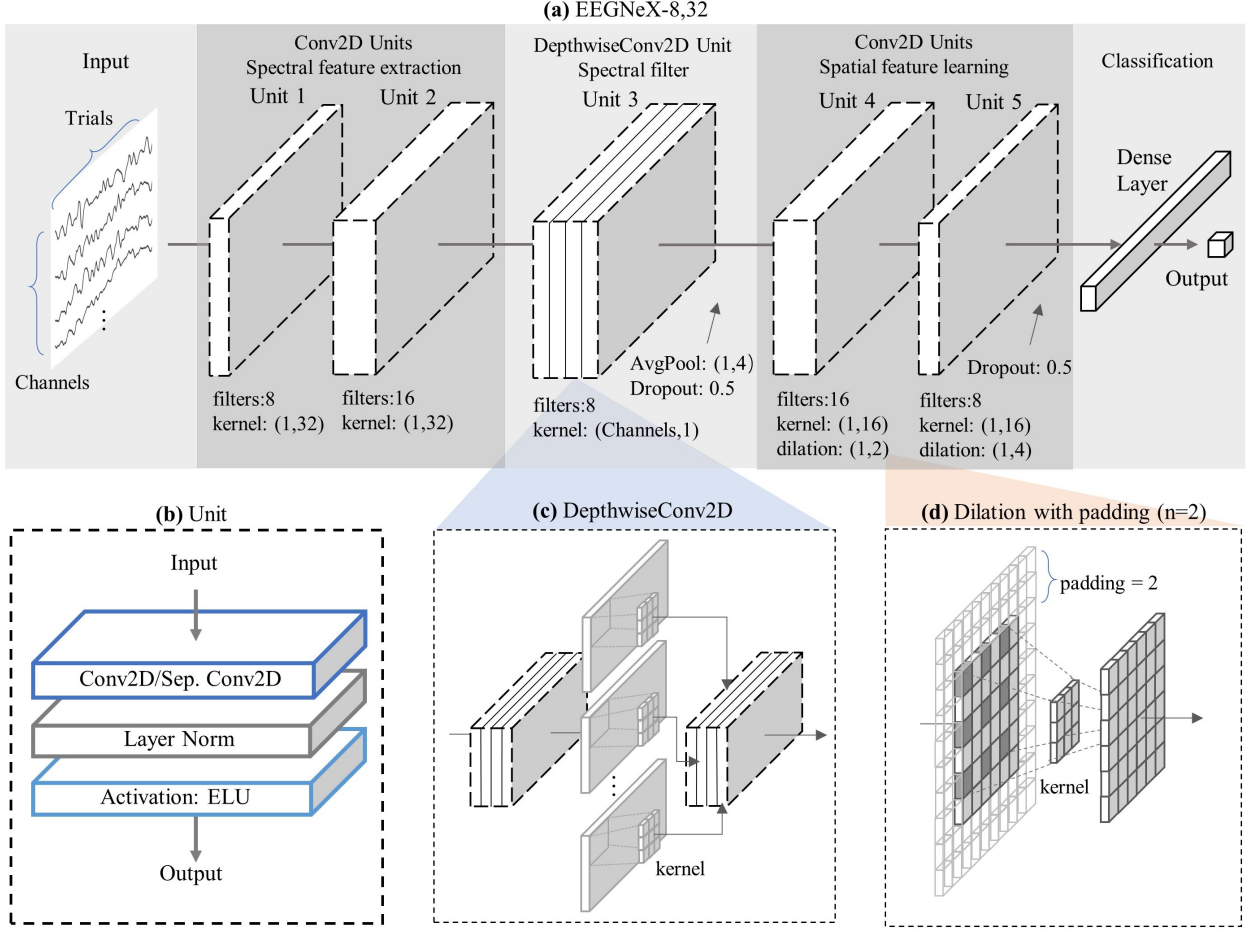


Figure 4: EEGNeX architecture; (a) the general structure visualization of EEGNeX-8,32. An EEGNeX is composed of five units. 8 means the number of temporal filters, while 32 stands for the kernel size; (b) The structure of the unit, which consists of a convolutional layer, a LayerNormalization layer, and an ELU activation layer; (c) The illustrative process of Depth-wise Convolution. In EEGNeX, it acts as a frequency spatial learner/filter. (d) Visualization of dilation mechanism: the kernel scans the convolution layer with spaces in-between to increase the kernel receptive field.

A characteristic overview of all datasets is presented in Table 3, with detailed descriptions and preprocessing procedures in Appendix.

All datasets are tested with candidate models for 10 rounds under the same train/validation/test ratio of 0.75/0.125/0.125 (training data size equivalent to 4-fold cross-validation test) with random split seeds each round, to observe their performance level and stability, as presented in Figure 5.

Across all datasets, the result validates the performance novelty of EEGNeX: in diverse EEG-classification tasks, EEGNeX competes favorably with EEGNet and outperforms all benchmark methods ($p < 0.05$, Wilcoxon tests). The general structure modification of EEGNeX (increased layer depth, wider network, the replacement of pooling layers) and micro adjustment are universally valid for accuracy improvement.

Throughout validation datasets and the proven advance in EEGNeX, some shared information could be extracted based on the benchmark ranking result: In EEG classification tasks, the performance of CNN-based structure is generally better than hybrid-model approaches (CNNs with RNNs). In comparison, CNNs with time-domain representation design (1D CNNs, causal structure) and RNN-based models are less effective. Among different CNN variations, the depthwise layer contributes to the model with cross-channel spatial feature extraction & representation ability and leads to high-rank accuracy. In addition, due to larger spatial kernel receptive field, dilated convolution structure benefits the performance level and its stability improvement.

Block	Layer	# filters	size	# params	Output	Options
	Input				(C, T)	
	Reshape				(1, C, T)	
1	Conv2D	F_1	(1, 32)	$32 * F_1$	(F_1 , C, T)	use_bias = False, padding='same'
	LayerNorm			$2 * T$	(F_1 , C, T)	
	Activation				(F_1 , C, T)	ELU
2	Conv2D	$F_1 * 4$	(1, 32)	$32 * F_1 * 16$	($F_1 * 4$, C, T)	use_bias = False, padding='same'
	LayerNorm			$2 * T$	($F_1 * 4$, C, T)	
	Activation				($F_1 * 4$, C, T)	ELU
3	DepthwiseConv2D	$F_1 * 4 * D$	(C, 1)	$2 * T$	($F_1 * 8$, 1, T)	depth_multiplier= D , use_bias = False, depthwise_constraint=max_norm(1.)
	LayerNorm			$2 * T$	($F_1 * 8$, 1, T)	
	Activation				($F_1 * 8$, 1, T)	ELU
	AvgPool2D		(1, 4)		($F_1 * 8$, 1, T/4)	
4	Dropout				($F_1 * 8$, 1, T/4)	rate = 0.5
	Conv2D	$F_1 * 4 * D$	(1, 16)	$16 * F_1 * 128 / 4$	($F_1 * 8$, 1, T/4)	use_bias = False, padding='same', dilation_rate=(1, 2)
	LayerNorm			$2 * T / 4$	($F_1 * 8$, 1, T/4)	
	Activation				($F_1 * 8$, 1, T/4)	ELU
5	Conv2D	F_1	(1, 16)	$16 * F_1 * 16 / 4$	(F_1 , 1, T/4)	use_bias = False, padding='same', dilation_rate=(1, 4)
	LayerNorm			$2 * T / 4$	(F_1 , 1, T/4)	
	Activation				(F_1 , 1, T/4)	
	Dropout				(F_1 , 1, T/4)	rate = 0.5
Classifier	Flatten			$F_1 * T / 4$	($F_1 * T / 4$)	
	Dense				N	kernel_constraint=max_norm(0.25)
	Activation				N	softmax

Table 2: EEGNeX-8,32 architecture, where C=number of channels, T=number of timesteps, F_1 = number of temporal filters (8), D=depth multiplier in DepthwiseConv2D (2), and N=number of classes, respectively.

Dataset	Subjects	Trials	Classes	Channels	Class Imbalance?	Size
MNIST of BRAIN DIGITS (MBD)	1	224	10	14	No	(64302, 14, 224)
OpenMBI Data (MBI)	54	200	2	20	No	(10800, 20, 512)
BCIC-IV-2A Data (SMR)	9	500	4	25	No	(2592, 25, 500)
Feedback Error-Related Negativity (ERN)	26	160	2	56	Yes, ~3.4:1	(5440, 56, 160)

Table 3: Description of experiment dataset collections. Class imbalance, if present, is given as odds, means different classes have uneven odds, which is given as the average class imbalance over all subjects.

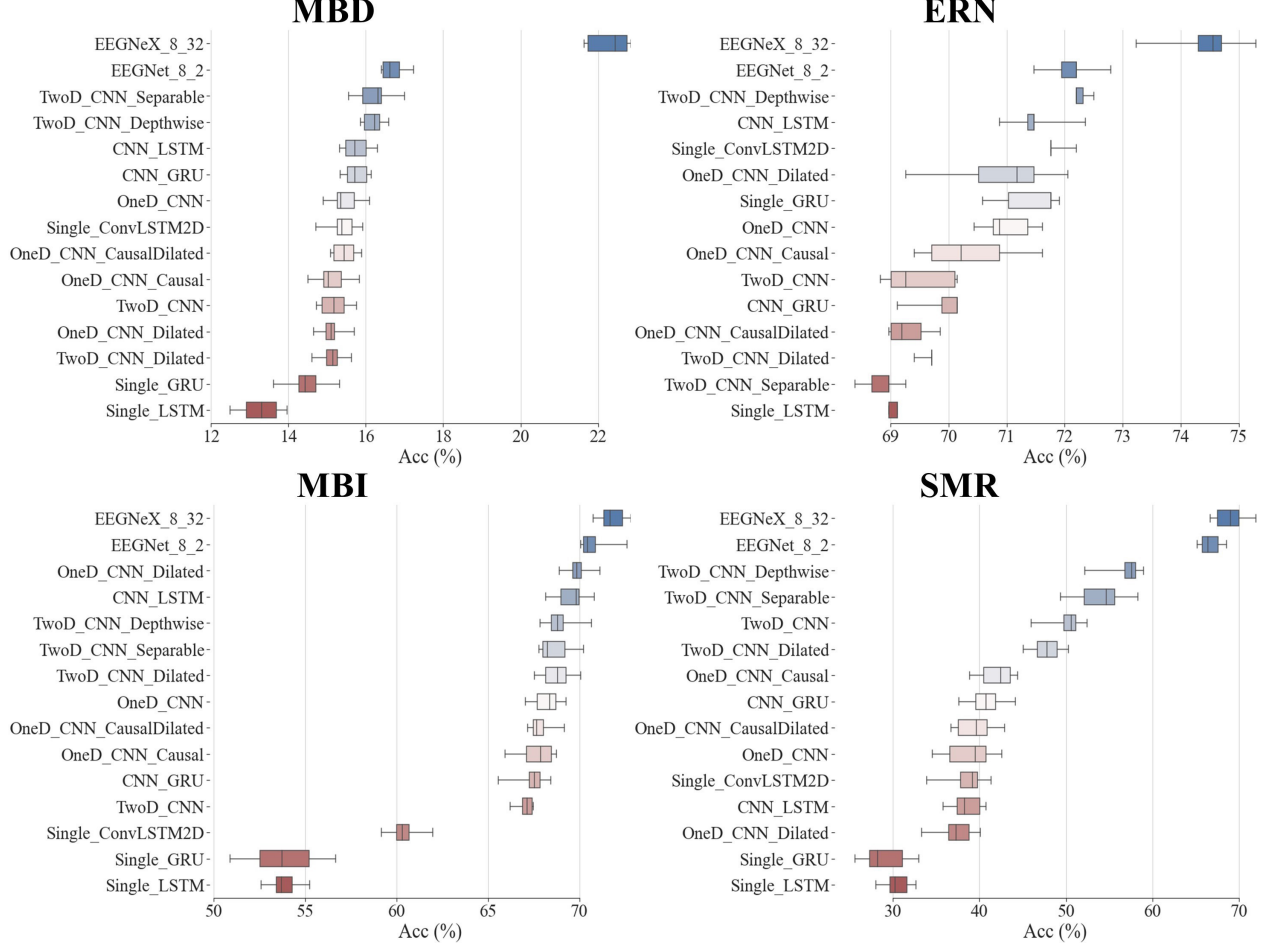


Figure 5: Classification accuracy for each dataset with candidate models in 10 rounds of random train/test:0.75/0.25 split. EEGNeX-8,32 owns dominant accuracy with stable performance across different tasks. In general, CNN-based models perform in high rank, especially ones with depthwise layer, followed by hybrid-model approaches and RNN-based models.

We also observed that in EEG-MI classification, the performance gap between different modeling architectures is significantly wider, especially between RNN-based methods and CNN-based methods.

4 Discussion

The thought in our brain, has been using mainly language to interact with the world for a long period. Just as Ludwig Josef Johann Wittgenstein [Wittgenstein, 2013] described:

“The limits of my language mean the limits of my world.”

Now, the BCI study creates a direct communication pathway for decoding brain’s activities, revealing a huge potential for establishing new patterns for human-computer interaction (HCI). By the generalization power of NNs, we foresee that the effort invested in interpreting brain activities would benefit a broad branch of domains, from information & communications technology to medical, from social science to design, and even revolutionize how we percept and understand reality. Take the design domain as an example; new BCI patterns would efficiently assist designers in expressing and interacting with the design work: their personal preferences, less expressible feelings, and subconscious perceptions can be captured, represented, and transferred more seamlessly via brain’s electrical signals without explicitly formalizing in languages or actions. Starting with the EEG classification, this study aims to minimize the gap between the BCI domain study and efficient NNs implementation. The benchmark offers a testbed for different network

architectures comparison, to encourage more interdisciplinary research participation. From this perspective, the construction of our open-source testbed remains primitive.

Based on the analysis result within the scope of this study, it is natural to conclude: the design of RNN-based and time-domain architecture of NN models is practically less efficient in EEG information representation than CNNs. In other words, NN techniques designed for local attention in sequential information decoding are generally not as efficient as global information extraction by moving receptive fields. The depthwise layer with enhanced performance further corroborates this viewpoint.

The limitation of this study is: The intention of designing this benchmark is to include diverse NN architectures in the research of reliable EEG signal decoding paths. We referred to the ConvNeXt to find the path shortcut for improved efficiency by the convolution inductive bias. Although the original paper of ConvNeXt claims the performance advance in the CV domain, image classification tasks than Transformer, the contribution of the self-attention mechanism is still worth investigating in the BCI domain. Besides the performance advance of CNN-based methods, we noticed from the benchmark result that the hybrid-model approach owns accuracy improvement than single architecture from its composition, which reveals a deeper EEG representation question. The reason is that the BCI signal data, in essential, combines characteristics from both the sequential format of NLP and the multi-channels from image data in CV. We observed several research attempts to adopt the BCI data in both branches [Craik et al., 2019, Hosseini et al., 2020]. In this context, the hybrid-model approach by deeply combining CNN and RNN architecture, the decent design of acquiring long-range global features in sequence by self-attention in Transformer, dimension reduction by encoder-decoder, and more NN techniques own potential for further improvement.

When aiming for a generalization of EEGNeX, it might be ideal for future research to test the decoding performance of EEGNeX using time series data from other imaging modalities, such as magnetoencephalography (MEG) and functional near-infrared spectroscopy (fNIRS). For the utility, it is worth mentioning that although the model is developed based on the EEG task challenges. The benchmark methods and the improvement conducted in the EEGNeX architecture rarely encode know-how feature engineering in the EEG domain specifically. Broader test scenarios within the scope of biological signal decoding in BCI topics could also benefit from this study.

5 Conclusion

In this study, we conduct large-scale benchmark neural network representations to test their performance for BCI. The classification accuracy and EEG information representation ability of neural networks with different structures were sorted out by comparing the results.

Based on the benchmark results, we propose a novel architecture: EEGNeX. Improvements are mainly adopted from neural network representation studies. We tested the EEGNeX in diverse EEG classification tasks to validate its universal adaptability. Since the performance improvement is less benefited by case-specific designs, EEGNeX owns the flexibility to combine with knowledge-based, domain feature engineering for variate scenarios adaptations. We hope that the results reported in this study and the benchmark will alleviate the difficulties of model implementation in various BCI studies and accelerate the path toward the representation study in this domain.

6 Appendix

6.1 Evaluation Dataset description

OpenBMI Data

A BCI dataset contains 2-class EEG data from 54 healthy subjects with MI of left/right-hand classes in total of 100 trials for each session in the length of 4s [Lee et al., 2019]. The original data is recorded at 1000Hz using 62 electrodes. As suggested by the original work, we selected 20 channels (FC-5/3/1/2/4/6, C-5/3/1/z/2/4/6, and CP-5/3/1/z/2/4/6) for the classification task. The EEG data is filtered with a notch of 1-40Hz and down-sampled at 128Hz.

BCIC-IV-2A Data

This dataset consists of 22 EEG channels and 3 EOG channels from 9 subjects with the task of 4-class motor imagery (left hand, right hand, feet, tongue) classification [Tangermann et al., 2012]. The sampling rate is 250 Hz with 0.5-100Hz notch filtered. In our analysis, we used all channel signals with the entire trial.

Feedback Error-Related Negativity (ERN) Data

Detecting the ERN feedback helps to improve the performance of the P300 speller in the application. The dataset is used in the “BCI Challenge” to determine whether the P300 feedback is correct (2-class classification task), hosted by Kaggle [Margaux et al., 2012] , consists of 26 healthy participants in 56 passive Ag/AgCl EEG sensors. The data is originally recorded at 600Hz, we used a 1-40Hz notch filter with 128Hz down-sampling for analysis.

6.2 Benchmark model structures

Single_GRU	Single_LSTM			Options
Layer	Layer	# units	size	
Input	Input		/	
GRU	LSTM	100	/	return_sequences=True, kernel_regularizer=l2(0.0001)
GRU	LSTM	100	/	return_sequences=True, kernel_regularizer=l2(0.0001)
GRU	LSTM	100	/	kernel_regularizer=l2(0.0001)
Dropout	Dropout		/	rate = 0.5
Dense	Dense	100	/	activation='elu'
Dense	Dense		/	activation='softmax'

Table 4: The architecture of GRU and LSTM; They both share the same general structure but with different RNN layer.

			1D_CNN	1D_CNN_Dilated	1D_CNN_Causal	1D_CNN_CausalDilated
Layer	# filters	size	Options	Options	Options	Options
Input						
Conv1D	64	3	/	/	padding='causal'	padding='causal'
BatchNorm						
Activation			elu			
Conv1D	64	3	/	dilation_rate=2	padding='causal'	padding='causal', dilation_rate=2
BatchNorm						
Activation			elu			
Conv1D	64	3	/	/	padding='causal'	padding='causal'
BatchNorm						
Activation			elu			
Dropout			rate = 0.5			
MaxPooling1D			pool_size=2			
Flatten						
Dense	100		activation='elu'			
Dense			activation='softmax'			

Table 5: The architecture of 1D CNN models; They share the same general structure but with different layer parameter options.

			2D_CNN	2D_CNN_Dilated
Layer	# filters	size	Options	Options
Input				
Conv2D	64	(1, 3)		
BatchNorm				
Activation			elu	
Conv2D	64	(1, 3)	/	dilation_rate=2
BatchNorm				
Activation			elu	
Conv2D	64	(1, 3)		
BatchNorm				
Activation			elu	
Dropout			rate = 0.5	
AvgPooling2D			pool_size=2, padding='same'	
Flatten				
Dense	100		activation='elu'	
Dense			activation='softmax'	

Table 6: The architecture of 2D CNN models; They share the same general structure but with different layer parameter setting options.

2D_CNN_Depthwise	2D_CNN_Separable			
Layer	Layer	# filters	size	Options
Input	Input			
DepthwiseConv2D	SeparableConv2D	64	(1, 3)	
BatchNorm	BatchNorm			
Activation	Activation			elu
SeparableConv2D	SeparableConv2D	64	(1, 3)	
BatchNorm	BatchNorm			
Activation	Activation			elu
SeparableConv2D	SeparableConv2D	64	(1, 3)	
BatchNorm	BatchNorm			
Activation	Activation			elu
Dropout	Dropout			rate = 0.5
AvgPooling2D	AvgPooling2D			pool_size=2, padding='same'
Flatten	Flatten			
Dense	Dense	100		activation='elu'
Dense	Dense			activation='softmax'

Table 7: The architecture of Depthwise and Separable 2D CNN.

Single_ConvLSTM2D			
Layer	# filters	size	Options
Input			
ConvLSTM2D	64	(1,3)	kernel_regularizer=l2(0.0001)
BatchNorm			
Activation			elu
Dropout			
Flatten			
Dense	100		activation='elu'
Dense			activation='softmax'

Table 8: The architecture of single 2D CNN with LSTM layer.

CNN_GRU	CNN_LSTM			
Layer	Layer	# filters	size	Options
Input	Input			TimeDistributed
Conv1D	Conv1D	64	3	TimeDistributed
BatchNorm	BatchNorm			
Activation	Activation			elu
Conv1D	Conv1D	64	3	TimeDistributed
BatchNorm	BatchNorm			
Activation	Activation			elu
Conv1D	Conv1D	64	3	TimeDistributed
BatchNorm	BatchNorm			
Activation	Activation			elu
Dropout	Dropout			TimeDistributed, rate = 0.5
MaxPooling1D	MaxPooling1D			TimeDistributed, pool_size=2
Flatten	Flatten			TimeDistributed
GRU	LSTM	480		kernel_regularizer=l2(0.0001)
Dropout	Dropout			rate = 0.5
Dense	Dense	100		activation='elu'
Dense	Dense			activation='softmax'

Table 9: The architecture of hybrid-models; They both share the same general structure but with different RNN layer.

Model	Accuracy									
Single_LSTM	13.33	13.25	13.82	12.80	12.49	12.81	13.28	13.96	13.65	13.70
Single_GRU	15.32	14.27	15.10	14.15	14.60	14.74	14.27	14.27	13.62	14.59
OneD_CNN	15.30	15.57	15.25	14.90	15.39	16.05	16.09	14.91	15.75	15.30
OneD_CNN_Dilated	15.18	14.91	14.99	15.04	15.18	14.97	15.71	15.19	15.25	14.65
OneD_CNN_Causal	15.71	14.94	14.90	15.13	15.21	14.51	14.54	15.83	14.94	15.43
OneD_CNN_CausalDilated	15.13	15.89	15.10	15.43	15.46	15.08	15.77	15.50	15.30	15.75
TwoD_CNN	14.73	15.72	15.77	15.10	15.39	15.01	15.25	14.82	14.74	15.46
TwoD_CNN_Dilated	14.60	15.49	15.13	15.18	15.22	14.91	15.63	15.07	14.96	15.27
TwoD_CNN_Separable	17.00	15.55	16.39	16.86	16.33	16.08	15.86	15.86	16.30	16.40
TwoD_CNN_Depthwise	16.36	16.34	16.34	15.86	15.89	16.11	15.95	15.99	16.59	16.58
CNN_LSTM	16.30	16.02	15.99	15.69	15.43	15.67	16.17	15.36	15.32	15.75
CNN_GRU	15.75	15.66	15.36	15.67	15.92	16.14	15.49	16.06	15.33	16.14
Single_ConvLSTM2D	15.25	15.41	14.71	15.35	15.71	15.67	15.92	15.53	15.32	14.97
EEGNet-8,2	16.53	16.92	16.40	16.42	16.72	16.70	17.07	17.23	16.53	16.42
EEGNeX-8,32	22.85	22.63	22.90	22.45	22.46	22.44	22.05	21.65	21.73	21.65

Table 10: 10-rounds model accuracy on MindBigData dataset.

References

Jonathan R Wolpaw, Niels Birbaumer, William J Heetderks, Dennis J McFarland, P Hunter Peckham, Gerwin Schalk, Emanuel Donchin, Louis A Quatrano, Charles J Robinson, Theresa M Vaughan, et al. Brain-computer interface technology: a review of the first international meeting. *IEEE transactions on rehabilitation engineering*, 8(2):164–173, 2000.

Jürgen Schmidhuber. Deep learning in neural networks: An overview. *Neural networks*, 61:85–117, 2015.

Uri Hasson, Samuel A Nastase, and Ariel Goldstein. Direct fit to nature: an evolutionary perspective on biological and artificial neural networks. *Neuron*, 105(3):416–434, 2020.

Ernst Niedermeyer and FH Lopes da Silva. *Electroencephalography: basic principles, clinical applications, and related fields*. Lippincott Williams & Wilkins, 2005.

Sepp Hochreiter and Jürgen Schmidhuber. Long short-term memory. *Neural computation*, 9(8):1735–1780, 1997.

Junyoung Chung, Caglar Gulcehre, KyungHyun Cho, and Yoshua Bengio. Empirical evaluation of gated recurrent neural networks on sequence modeling. *arXiv preprint arXiv:1412.3555*, 2014.

Giulio Ruffini, David Ibanez, Marta Castellano, Stephen Dunne, and Aureli Soria-Frisch. Eeg-driven rnn classification for prognosis of neurodegeneration in at-risk patients. In *International Conference on Artificial Neural Networks*, pages 306–313. Springer, 2016.

Alexander Craik, Yongtian He, and Jose L Contreras-Vidal. Deep learning for electroencephalogram (eeg) classification tasks: a review. *Journal of neural engineering*, 16(3):031001, 2019.

Laith Alzubaidi, Jinglan Zhang, Amjad J Humaidi, Ayad Al-Dujaili, Ye Duan, Omran Al-Shamma, José Santamaría, Mohammed A Fadhel, Muthana Al-Amidie, and Laith Farhan. Review of deep learning: Concepts, cnn architectures, challenges, applications, future directions. *Journal of big Data*, 8(1):1–74, 2021.

Hamdi Altaheri, Ghulam Muhammad, Mansour Alsulaiman, Syed Umar Amin, Ghadir Ali Altuwajri, Wadood Abdul, Mohamed A Bencherif, and Mohammed Faisal. Deep learning techniques for classification of electroencephalogram (eeg) motor imagery (mi) signals: a review. *Neural Computing and Applications*, pages 1–42, 2021.

Vernon J Lawhern, Amelia J Solon, Nicholas R Waytowich, Stephen M Gordon, Chou P Hung, and Brent J Lance. Eegnet: a compact convolutional neural network for eeg-based brain–computer interfaces. *Journal of neural engineering*, 15(5):056013, 2018.

Xin Deng, Boxian Zhang, Nian Yu, Ke Liu, and Kaiwei Sun. Advanced tsgl-eegnet for motor imagery eeg-based brain-computer interfaces. *IEEE Access*, 9:25118–25130, 2021.

Wenkai Huang, Yihao Xue, Lingkai Hu, and Hantang Liuli. S-eegnet: electroencephalogram signal classification based on a separable convolution neural network with bilinear interpolation. *IEEE Access*, 8:131636–131646, 2020.

Hubert Cecotti and Axel Graser. Convolutional neural networks for p300 detection with application to brain-computer interfaces. *IEEE transactions on pattern analysis and machine intelligence*, 33(3):433–445, 2010.

Robin Tibor Schirrmeister, Jost Tobias Springenberg, Lukas Dominique Josef Fiederer, Martin Glasstetter, Katharina Eggensperger, Michael Tangermann, Frank Hutter, Wolfram Burgard, and Tonio Ball. Deep learning with convolutional neural networks for eeg decoding and visualization. *Human brain mapping*, 38(11):5391–5420, 2017.

Zheng Yang Chin, Kai Keng Ang, Chuanchu Wang, Cuntai Guan, and Haihong Zhang. Multi-class filter bank common spatial pattern for four-class motor imagery bci. In *2009 Annual International Conference of the IEEE Engineering in Medicine and Biology Society*, pages 571–574. IEEE, 2009.

Mouad Riyad, Mohammed Khalil, and Abdellah Adib. Incep-eegnet: a convnet for motor imagery decoding. In *International Conference on Image and Signal Processing*, pages 103–111. Springer, 2020.

Ravikiran Mane, Effie Chew, Karen Chua, Kai Keng Ang, Neethu Robinson, A Prasad Vinod, Seong-Whan Lee, and Cuntai Guan. Fbcnet: A multi-view convolutional neural network for brain-computer interface. *arXiv preprint arXiv:2104.01233*, 2021.

Salma Alhagry, Aly Aly Fahmy, and Reda A El-Khoribi. Emotion recognition based on eeg using lstm recurrent neural network. *International Journal of Advanced Computer Science and Applications*, 8(10), 2017.

Ping Wang, Aimin Jiang, Xiaofeng Liu, Jing Shang, and Li Zhang. Lstm-based eeg classification in motor imagery tasks. *IEEE transactions on neural systems and rehabilitation engineering*, 26(11):2086–2095, 2018.

Ashish Vaswani, Noam Shazeer, Niki Parmar, Jakob Uszkoreit, Llion Jones, Aidan N Gomez, Łukasz Kaiser, and Illia Polosukhin. Attention is all you need. *Advances in neural information processing systems*, 30, 2017.

JX Chen, DM Jiang, and YN Zhang. A hierarchical bidirectional gru model with attention for eeg-based emotion classification. *IEEE Access*, 7:118530–118540, 2019.

Theerawit Wilaiprasitporn, Apiwat Ditthapron, Karis Matchaparn, Tanaboon Tongbuasirilai, Nannapas Banluesombatkul, and Ekapol Chuangsuwanich. Affective eeg-based person identification using the deep learning approach. *IEEE Transactions on Cognitive and Developmental Systems*, 12(3):486–496, 2019.

Jacob Devlin, Ming-Wei Chang, Kenton Lee, and Kristina Toutanova. Bert: Pre-training of deep bidirectional transformers for language understanding. *arXiv preprint arXiv:1810.04805*, 2018.

Alexey Dosovitskiy, Lucas Beyer, Alexander Kolesnikov, Dirk Weissenborn, Xiaohua Zhai, Thomas Unterthiner, Mostafa Dehghani, Matthias Minderer, Georg Heigold, Sylvain Gelly, et al. An image is worth 16x16 words: Transformers for image recognition at scale. *arXiv preprint arXiv:2010.11929*, 2020.

Karen Simonyan and Andrew Zisserman. Very deep convolutional networks for large-scale image recognition. *arXiv preprint arXiv:1409.1556*, 2014.

Kaiming He, Xiangyu Zhang, Shaoqing Ren, and Jian Sun. Deep residual learning for image recognition. In *Proceedings of the IEEE conference on computer vision and pattern recognition*, pages 770–778, 2016.

Mingxing Tan and Quoc Le. Efficientnet: Rethinking model scaling for convolutional neural networks. In *International conference on machine learning*, pages 6105–6114. PMLR, 2019.

Zhuang Liu, Hanzi Mao, Chao-Yuan Wu, Christoph Feichtenhofer, Trevor Darrell, and Saining Xie. A convnet for the 2020s. In *Proceedings of the IEEE/CVF Conference on Computer Vision and Pattern Recognition*, pages 11976–11986, 2022.

D. Vivancos. Mindbigdata the 'mnist' of brain digits. URL <http://www.mindbigdata.com/opendb/>.

Martín Abadi, Ashish Agarwal, Paul Barham, Eugene Brevdo, Zhifeng Chen, Craig Citro, Greg S Corrado, Andy Davis, Jeffrey Dean, Matthieu Devin, et al. Tensorflow: Large-scale machine learning on heterogeneous distributed systems. *arXiv preprint arXiv:1603.04467*, 2016.

Mohammad-Parsa Hosseini, Amin Hosseini, and Kiarash Ahi. A review on machine learning for eeg signal processing in bioengineering. *IEEE reviews in biomedical engineering*, 14:204–218, 2020.

Sergey Ioffe and Christian Szegedy. Batch normalization: Accelerating deep network training by reducing internal covariate shift. In *International conference on machine learning*, pages 448–456. PMLR, 2015.

Anish Shah, Eashan Kadam, Hena Shah, Sameer Shinde, and Sandip Shingade. Deep residual networks with exponential linear unit. In *Proceedings of the third international symposium on computer vision and the internet*, pages 59–65, 2016.

François Chollet. Xception: Deep learning with depthwise separable convolutions. In *Proceedings of the IEEE conference on computer vision and pattern recognition*, pages 1251–1258, 2017.

Aaron van den Oord, Sander Dieleman, Heiga Zen, Karen Simonyan, Oriol Vinyals, Alex Graves, Nal Kalchbrenner, Andrew Senior, and Koray Kavukcuoglu. Wavenet: A generative model for raw audio. *arXiv preprint arXiv:1609.03499*, 2016.

Andrew G Howard, Menglong Zhu, Bo Chen, Dmitry Kalenichenko, Weijun Wang, Tobias Weyand, Marco Andreetto, and Hartwig Adam. Mobilenets: Efficient convolutional neural networks for mobile vision applications. *arXiv preprint arXiv:1704.04861*, 2017.

Dominik Scherer, Andreas Müller, and Sven Behnke. Evaluation of pooling operations in convolutional architectures for object recognition. In *International conference on artificial neural networks*, pages 92–101. Springer, 2010.

Mark Sandler, Andrew Howard, Menglong Zhu, Andrey Zhmoginov, and Liang-Chieh Chen. Mobilenetv2: Inverted residuals and linear bottlenecks. In *Proceedings of the IEEE conference on computer vision and pattern recognition*, pages 4510–4520, 2018.

Min-Ho Lee, O-Yeon Kwon, Yong-Jeong Kim, Hong-Kyung Kim, Young-Eun Lee, John Williamson, Siamac Fazli, and Seong-Whan Lee. Eeg dataset and openbmi toolbox for three bci paradigms: An investigation into bci illiteracy. *GigaScience*, 8(5):giz002, 2019.

Michael Tangermann, Klaus-Robert Müller, Ad Aertsen, Niels Birbaumer, Christoph Braun, Clemens Brunner, Robert Leeb, Carsten Mehring, Kai J Miller, Gernot Mueller-Putz, et al. Review of the bci competition iv. *Frontiers in neuroscience*, page 55, 2012.

Perrin Margaux, Maby Emmanuel, Daligault Sébastien, Bertrand Olivier, and Mattout Jérémie. Objective and subjective evaluation of online error correction during p300-based spelling. *Advances in Human-Computer Interaction*, 2012, 2012.

Ludwig Wittgenstein. *Tractatus logico-philosophicus*. Routledge, 2013.